

# UAS Reliability and Risk Analysis

Christopher W. Lum and Dai A. Tsukada

William E. Boeing Department of Aeronautics & Astronautics, University of Washington, Seattle, WA, USA

---

1 Introduction	1
2 Motivation for Risk Analysis	1
3 Risk Factors	2
4 Risk Model	3
5 Example Calculations	5
6 Conclusion	9
Notation and Nomenclature	10
References	10

---

## 1 INTRODUCTION

The past several decades have seen significant advances in UAS technology (see Unmanned Aerial Vehicles (UAVs)). In the last 10 years, there has been a corresponding increase in their use by military organizations around the world. Recently, the utilization of these technologies has begun to grow beyond the military domain with an increased interest in civilian and commercial applications. Recent market analysis shows evidence for exponential growth and utilization of UAS in the future (U.S. Department of Transportation, 2013). This increased usage will result in complex interactions between UAS and general aviation and commercial flights. UAS missions must be able to achieve an acceptable level of safety and reliability when accessing the National Airspace System (NAS). Reliable and realistic methods of evaluating risk must be developed in order to allow further development and use of UAS while ensuring public safety. After examining several risk factors, this

chapter will present a simplified model to assess and predict the risk associated with a given UAS operation.

Several efforts have been made in the past to analyze the risk of a UAS operation. One of the first efforts involved modeling midair collisions of manned aircraft using random collision theory and comparing results to historical data (Anno, 1982). Similar work was performed by McGeer with extensions involving regulatory policy and economics of these systems (McGeer, 1994). More recently, the focus has shifted toward integrating UAS into the NAS. Weibel and Hansman performed risk analysis of UAS operation in the NAS by combining the severity of the hazard and its likelihood of occurrence (Weibel and Hansman, 2005). A risk-based approach to analyze the safety of UAS operations was examined at North Carolina State University in the development of the System-Level Airworthiness Tool (SLAT) (Burke, 2010). Groups such as Clothier *et al.* have developed models such as the barrier-bow-tie model to identify and manage risk (Clothier *et al.*, 2015, 2015, 2015; Williams *et al.*, 2014). A simplified risk assessment framework and tool was developed to enable UAS manufacturers and operators to quantitatively evaluate risk of a mission in terms of human safety (Lum and Waggoner, 2011; Lum *et al.*, 2011). In the previous works, the authors focus on the expected number of fatalities per flight hour as the primary safety metric.

## 2 MOTIVATION FOR RISK ANALYSIS

It is generally perceived that there are a number of obstacles to the full integration of UAS into the NAS. The Federal Aviation Administration (FAA) has identified, in the UAS–NAS

integration roadmap, that the most pressing technological challenges are “sense-and-avoid” (SAA) capability and command-and-control (C2) link reliability (Federal Aviation Administration, 2013). Since the operator of a UAS is not able to provide the “see-and-avoid” ability of which an onboard pilot is capable, the development of reliable SAA technology is essential for UAS to gain full airspace access (Anon, 2011).

Although the most UA possess low-level autonomy, a reliable communication link between the UA and the ground control station is often necessary for high-level control such as navigation, tasking, and air-traffic control. In addition to improving the C2 link reliability, regulations and protocols must be established to ensure safe and predictable behavior in the case of a lost link due to situations such as equipment failure or malicious jamming.

Thoroughly addressing these issues so that UAS may be routinely and safely incorporated throughout the NAS will take years. In the meantime, standards and tools need to be developed that will “enable the widest range of activity that can be safely conducted within the shortest rulemaking timeframe” (ASTM F38 Committee).

The risk assessment tool presented here aims to provide UAS operators and airspace regulators with a simplified and trustworthy method of evaluating the safety of proposed UAS operations. The model in this framework is first and foremost concerned with estimating the potential risk to human safety both aboard other aircraft and on the ground, and does not take into account the potentially significant economic risk associated with a mission.

## 3 RISK FACTORS

There are numerous ways in which a UAS may fail and many incidents are the result of multiple factors. These causes may be grouped into several categories such as operator error, improper maintenance, equipment failure, weather, and bird strike. Understanding each risk factor and its ramification is necessary to conduct an accurate risk assessment. Having a thorough understanding of risk factors also helps to improve the reliability of the UAS, as it allows operators and regulators to address each factor individually, and understand how failure rates might be lowered over time. In the following section, several risk factors specific to certain operational time and flight phase are discussed.

### 3.1 System failure

System failure is a broad term that may encompass several factors. A hardware or mechanical failure (including engine

failure, loss of link, or damage to control surface) could lead to unintended or abnormal system behavior. Hazards could also arise from software failures such as a flight computer failure or a ground control station failure. Given the wide taxonomy of UAS, enumerating and evaluating each individual failure is not practical and therefore we adopt the use of the general system failure designation. Referring to the historical data is one approach to estimate system failure rate of the UAS. For example, the Air Force Class A Aerospace Mishap records, maintained by the Judge Advocate General’s office, are a useful resource for tracking the distribution of mishap causes over time for a particular aircraft system (Accident Investigation Board, n.d.). Another way of estimating failure rate is to note the failure rate of each subcomponent using reliability analyses such as failure modes, effects, and criticality analysis (FMECA) (U.S. Department of Defense, 1980). These analyses are effective especially when the system is relatively new and no historical data is available.

### 3.2 Human error

Human error is another major risk factor for UAS operation. This includes inadequate operator response, mission planning error, or improper maintenance of the UAS. A recent study of Predator mishaps conducted by the Air Force Research Laboratory revealed that after system failures that happen in the first several years of operation are addressed and mitigated, the dominant risk factor becomes various human errors (Herz, 2008). These risks can be mitigated by refocusing on the training of the new and current operators.

### 3.3 Bird strikes

Although the model considered here does not distinguish between mishaps in different phases of flight, it is noteworthy that bird strike is one of the greatest risk for aircrafts during taxi, takeoff, and landing phase, with 80% occurring below 305 m (1000 ft) AGL and 96% occurring below 1542 m (5000 ft) AGL (Dolbeer *et al.*, 2009). For general aviation and commercial flights, these altitudes are only encountered during landing and takeoff. Combining this with the fact that operating areas during these phases of flight are typically near airports or otherwise controlled areas, it is reasonable to assume that bird strikes only pose a nontrivial threat to people onboard aircraft as opposed to those on the ground. This assumption may not be valid for UAS operations given that the majority of these operations are currently below 400’ AGL. While the current model neglects bird strikes, this

factor should be considered as a potentially nontrivial risk associated with UAS operations in the future.

## 4 RISK MODEL

The risk to human safety in this model stems from two potential causes: midair collisions and ground collisions. For instance, if a UAS collides with a transient aircraft (e.g., commercial flights, regional jets, and general aviation), it may injure or kill the people onboard the transient aircraft. Both of these vehicles will then create debris that has potential to affect bystanders on the ground. The model aims to quantify the risk to human life by estimating fatalities per flight hour due to these factors.

### 4.1 Midair collisions

A midair collision is further separated into two categories. The first category models collisions of a UAS with other transient aircraft (denoted as transient collisions) and the second is collision of UAS with other UAS within their same fleet (denoted as in-fleet collisions). For both cases, unmitigated collision rates are modeled using a Maxwell molecule formulation (McQuarrie and Simon, 1997). This theory was similarly applied to air traffic in prior literature (Anno, 1982; McGeer, 1994; Vagners *et al.*, 1999).

#### 4.1.1 Transient collisions

The collision frequency between a single UA and transient air traffic is a product of the transient aircraft density, the combined frontal areas, and the velocity of both the UA and the transient aircraft. We define  $\rho_O$  to be the density of transient aircraft per  $\text{km}^3$ ,  $\phi_O$  and  $\phi_{ua}$  to be the frontal area in  $\text{km}^2$  of the transient aircraft and the UA, and  $V_O$  and  $V_{ua}$  as the velocity in  $\text{km h}^{-1}$  of the transient aircraft and the UA. In

order to average the risk of a midair collision over all orientations, the frontal areas of the UA and the transient aircraft are recast as circles of radii  $R_{ua} = \sqrt{\phi_{ua}/\pi}$  (km) and  $R_O = \sqrt{\phi_O/\pi}$  (km). A collision occurs if the centers of the aircraft are within a distance  $R_{ua} + R_O$ . The instantaneous collision area is therefore,

$$\phi_{col} = \pi(R_{ua} + R_O)^2 = \phi_{ua} + \phi_O + 2\sqrt{\phi_{ua}\phi_O} \quad (1)$$

We start with a simplification that the transient aircraft are stationary ( $V_O = 0$ ), in which case the volume of collision airspace that the UA sweeps out in a time  $\Delta T$  is simply  $V_{col} = \phi_{col}V_{ua}\Delta T$ . The number of collisions is a product of the collision volume and the transient aircraft density. Dividing by the time  $\Delta T$  gives the expected collision rate for a single UA with stationary transient aircraft.

$$\widehat{F}_{transient} = \rho_O\phi_{col}V_{ua} \quad (2)$$

To correct for the fact that the transient aircraft are not stationary ( $V_O \neq 0$ ),  $V_{ua}$  is replaced with a relative velocity. In order to develop conservative model of collisions, we assume that all transient aircraft are flying directly at the UA that gives us the maximum (and conservative) relative velocity of  $V_{rel} = V_{ua} + V_O$ . Assuming that UA collisions are independent of each other, the total collision rate for the fleet of UA is simply obtained by multiplying Equation 2 by the number of UA in the fleet and replacing  $V_{ua}$  with  $V_{rel}$

$$\widehat{F}_{transient} = N_{ua}\rho_O\phi_{col}V_{rel} \quad (3)$$

Collision avoidance capabilities gained from the airspace structure, procedural separation, or SAA technologies are incorporated in the collision model using the parameter  $\epsilon$ , the probability that a given aircraft will avoid an imminent collision with another aircraft. This framework is explained in Figure 1. With this framework, the expected collision rate of the UA fleet and transient aircraft with collision avoidance

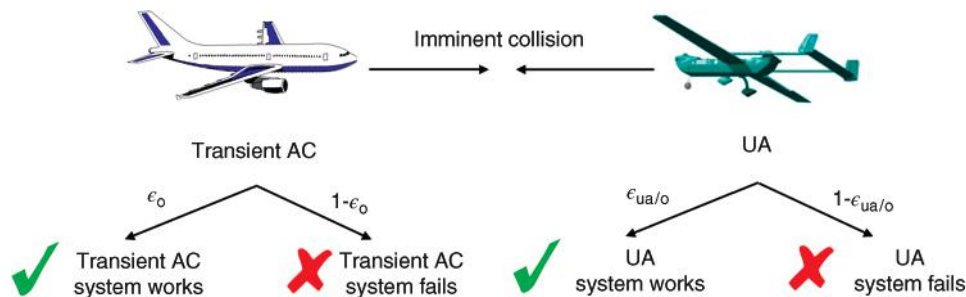


**Figure 1.** Collision avoidance framework. Both transient aircraft and UA collision avoidance must fail in order for a midair collision to occur.

## 4 Vehicle Design

taken into account is given by

$$F_{\text{transient}} = N_{\text{ua}} \rho_o \phi_{\text{col}} V_{\text{rel}} (1 - \varepsilon_{\text{ua/o}}) (1 - \varepsilon_o) \quad (4)$$

### 4.1.2 In-fleet collisions

A similar analysis can be performed to estimate collision rates of the second category, collision between UA within their own fleet. This involves using the previous equations with substitutions of  $V_O = V_{\text{ua}}$ ,  $\phi_O = \phi_{\text{ua}}$ , and  $\rho_O = \rho_{\text{ua}}$ . Previously, the density of transient aircraft was assumed to be uniformly spread over the operating volume. With in-fleet UA operations, there may be missions where the fleet of UAS are in close proximity to each other or otherwise spaced such that a uniform density over the entire operating volume is not a reasonable assumption. In order to take these factors into account, once the mission has been selected, the appropriate volumes are calculated using  $\eta_{\text{ops}} = A_{\text{ops}}(z_{\text{max}} - z_{\text{min}})$  and  $\eta_{\text{fleet}} = A_{\text{ops, fleet}}(z_{\text{max, fleet}} - z_{\text{min, fleet}})$ . The expected in-fleet collision rate is therefore

$$F_{\text{fleet}} = N_{\text{ua}} \rho_{\text{ua}} (4\phi_{\text{ua}}) (V_{\text{rel}}) (1 - \varepsilon_{\text{ua/ua}})^2 \quad (5)$$

The total number of midair collisions,  $\alpha$  (both between UA and transient aircraft and between UA and other UA), during a mission is simply the sum of  $F_{\text{transient}}$  and  $F_{\text{fleet}}$  multiplied by the mission duration,  $M_L$ .

$$\alpha = M_L (F_{\text{transient}} + F_{\text{fleet}}) \quad (6)$$

## 4.2 Ground collisions

Midair collisions are only a portion of the analysis. After midair collision or general system failure occurs, a risk to

pedestrians or bystanders on the ground still exists as the UA will fall to the ground and either strike a person or a building (the two scenarios considered in this model). The risk of ground collisions from crashes due to systems failures is found assuming that upon failure, the UA glides to the ground at maximum L/D (worst-case scenario) with glide angle  $\gamma$ . The associated geometry is shown in Figure 2.

The risk of ground collisions from midair collisions assumes upon midair collision, the UA will approach the surface in vertical free fall. The expected number of building and pedestrian strikes is composed of two calculations that take each case (glide and free fall) into account. For example, if the UA has a system failure and glides to the ground at the best glide angle, the collision areas in  $\text{km}^2$  that the UA may strike are given by

$$A_{L_{H_p}} = (w_{\text{ua}} + 2R_p) \left( L_{\text{ua}} + \frac{H_p}{\tan \gamma} + 2R_p \right) \quad (7)$$

$$A_{L_{H_b}} = (w_{\text{ua}} + w_b) \left( L_{\text{ua}} + \frac{H_b}{\tan \gamma} + w_b \right) \quad (8)$$

In a similar fashion, if the UA sustains a midair collision, it is assumed that it will fall vertically to the ground. In this case, the collision areas in  $\text{km}^2$  become

$$A_{L_{V_p}} = \pi \left( \frac{\max(w_{\text{ua}}, L_{\text{ua}})}{2} + R_p \right)^2 \quad (9)$$

$$A_{L_{V_b}} = \pi \left( \frac{\max(w_{\text{ua}}, L_{\text{ua}})}{2} + \frac{w_p}{2} \right)^2 \quad (10)$$

In Equations 7–10,  $w_b$  is the average building width in km (defined as  $w_b = \sqrt{A_b}$ , where  $A_b$  is the average building size

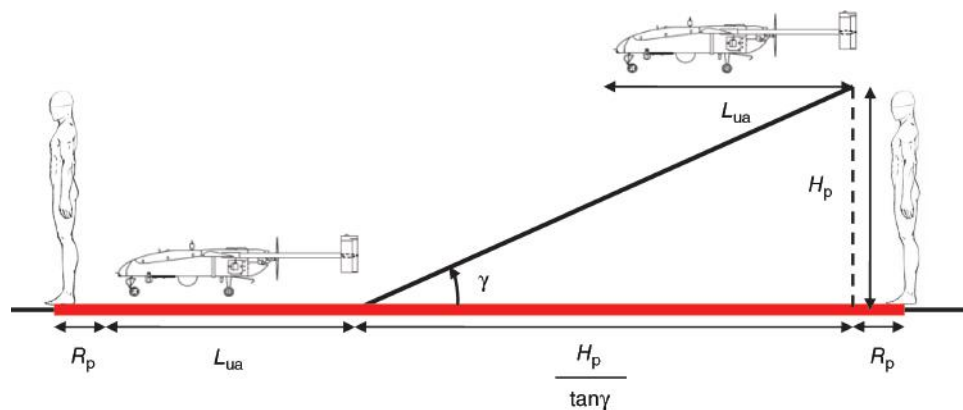


**Figure 2.** Geometry showing affected distance covered by UA during a horizontal, gliding crash. The total affected area is this distance multiplied by the wingspan of UA plus  $2R_p$ .

in  $\text{km}^2$ ),  $H_b$  is the average building height in km,  $R_p$  is the radius of a person,  $H_p$  is the height of a person,  $\gamma$  is the UA glide angle without power,  $w_{ua}$  is the UA wingspan in km, and  $L_{ua}$  is the UA length in km.

The numbers of aircraft crashes are a function of both  $F_{\text{transient}}$  and  $F_{\text{fleet}}$ . Since a single midair collision affects two aircraft, the rate of aircraft crashes (and subsequent ground strikes) per hour becomes

$$C_{\text{midair}} = 2(F_{\text{transient}} + F_{\text{fleet}}) \quad (11)$$

The number of pedestrian and building strikes per hour is a combination of system failures and midair collisions.

$$F_{\text{ped}} = F_{\text{ped,p}} + F_{\text{ped,midair}} = N_{\text{ua}}\lambda\sigma_p A_{L_{H_p}} + C_{\text{midair}}\sigma_p A_{L_{V_p}} \quad (12)$$

$$F_{\text{bldg}} = F_{\text{bldg,p}} + F_{\text{bldg,midair}} = N_{\text{ua}}\lambda\sigma_b A_{L_{H_b}} + C_{\text{midair}}\sigma_b A_{L_{V_b}} \quad (13)$$

In these expressions,  $\lambda$  is the UAS midair failure rate per hour from all sources for a single UA. This can be estimated by examining risk factors associated with UAS operation as described in previous section, or cited by manufacturers as the mean time between failures.  $\sigma_p$  and  $\sigma_b$  are the building and pedestrian densities (respectively) per  $\text{km}^2$ .

A successful risk assessment must communicate the results in a way that provides the user with a tangible sense for the risk involved. The most important result is the number of fatalities expected. Using previously obtained parameters, the expected number of fatalities per hour becomes

$$F_{\text{fat}} = F_{\text{fat,p}} + F_{\text{fat,midair}} \quad (14)$$

where

$$F_{\text{fat,p}} = F_{\text{ped,p}}D_{\text{ped}} + F_{\text{bldg,p}}D_{\text{bldg}}$$

and

$$F_{\text{fat,midair}} = F_{\text{ped,midair}}D_{\text{ped}} + F_{\text{bldg,midair}}P_O$$

In Equation 14,  $D_{\text{ped}}$  is the fatality rate for a pedestrian strike. It is defined as the average number of fatalities incurred when a UA strikes a pedestrian and is therefore in range of [0,1].  $D_{\text{bldg}}$  is the fatality rate for a building strike (in range of [0,all people in building]). This allows versatility in modeling hard structures where people are more protected versus softer structures such as residential homes.  $P_O$  is the average number of passengers on a transient aircraft. The model assumes that a collision between a UA and a transient aircraft causes the death of all passengers aboard the transient aircraft.

The risk model presented here was designed to be a conservative and easily accessible method to estimate the risk to human life incurred from a given UAS operation. The

capabilities of this model can be further extended by adding extra functionalities. For example, one can utilize this risk model to focus on assessing risk of a location specific mission by incorporating the probability distribution function (PDF) for impact near the operating area and the local bystander distribution obtained from census data or satellite imagery (Lum *et al.*, 2011). Although this requires an accurate understanding of the system through high-fidelity simulation or experimental data, the outcome will give a site-specific risk assessment.

## 5 EXAMPLE CALCULATIONS

This section presents example calculations of risk assessment for two scenarios. The first scenario is a mission that shows a potentially viable operation for UAS. The second scenario illustrates an operation that does not appear to be a good fit for utilizing UAS.

### 5.1 Scenario 1: environmental monitoring

Environmental monitoring has been a popular civilian application for UAS in recent years. UAS have been widely used to gather environmental data, assess damage from natural disasters, monitor wildfires, and perform aerial surveys (Lum *et al.*, 2005; Lum *et al.*, 2015; Lum and Vagners, 2009). As an example case, we will consider a team of small UAS taking part in environmental mapping for precision agriculture using multispectral camera over cropland. The risk assessment will be for mapping application, but the process is essentially the same for wildfire detection, search and rescue, or other low-altitude operations.

#### 5.1.1 UAS properties, operating area, and transient aircraft

For this scenario, we assume that the operator uses a Skywalker 1900 airframe with customized flight controller to operate as a UAS. By referencing pictures and diagrams of the Skywalker 1900, seen in Figure 3, the frontal area was estimated. The frontal area approximation is depicted in Figure 4.

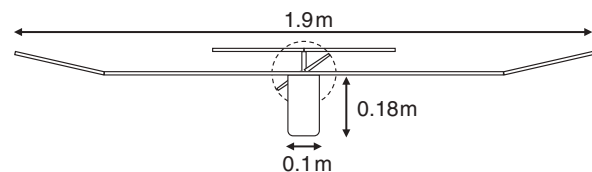


**Figure 3.** Skywalker 1900 frontal area geometries.

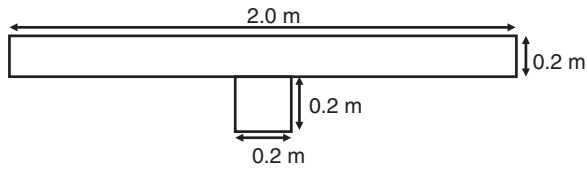


Figure 4. Skywalker 1900 frontal area approximation.

The Skywalker 1900 is dynamically stable and therefore without power, it will continue gliding at an estimated glide angle of  $5^\circ$ . We assume a mission length of 20 min with two aircraft operating simultaneously. In order to simulate the

worst-case scenario for system failure, we consider a case where flight computer fails and commands full throttle with a wings-level condition with a fully charged battery. We also assume that after the loss of battery, the aircraft continues gliding. Given that the nominal operational altitude of UAS is 122 m AGL, these give a maximum impact distance (assuming no wind) of 23.6 km. The impact distance geometry is seen in Figure 5. Based on the flight history, the system failure rate was conservatively estimated to be 0.1 per flight hour. Since it is a small aircraft, we assume no collision avoidance capability is available ( $\epsilon_{ua/o} = \epsilon_{ua/o} = 0$ ). Collision avoidance capability from transient aircraft is also assumed to be small ( $\epsilon_o = 0.05$ ) as the Skywalker 1900 is

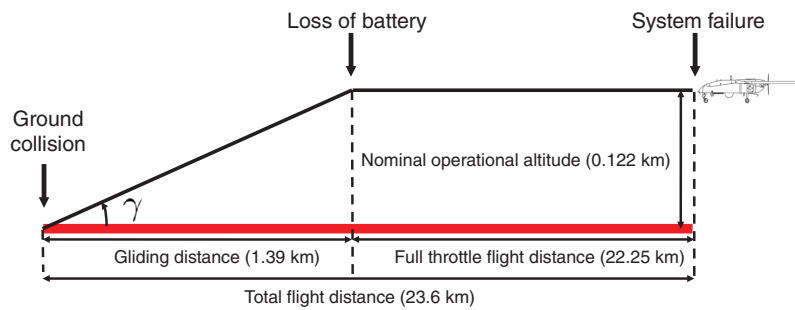


Figure 5. Maximum impact distance geometry for the worst-case scenario.

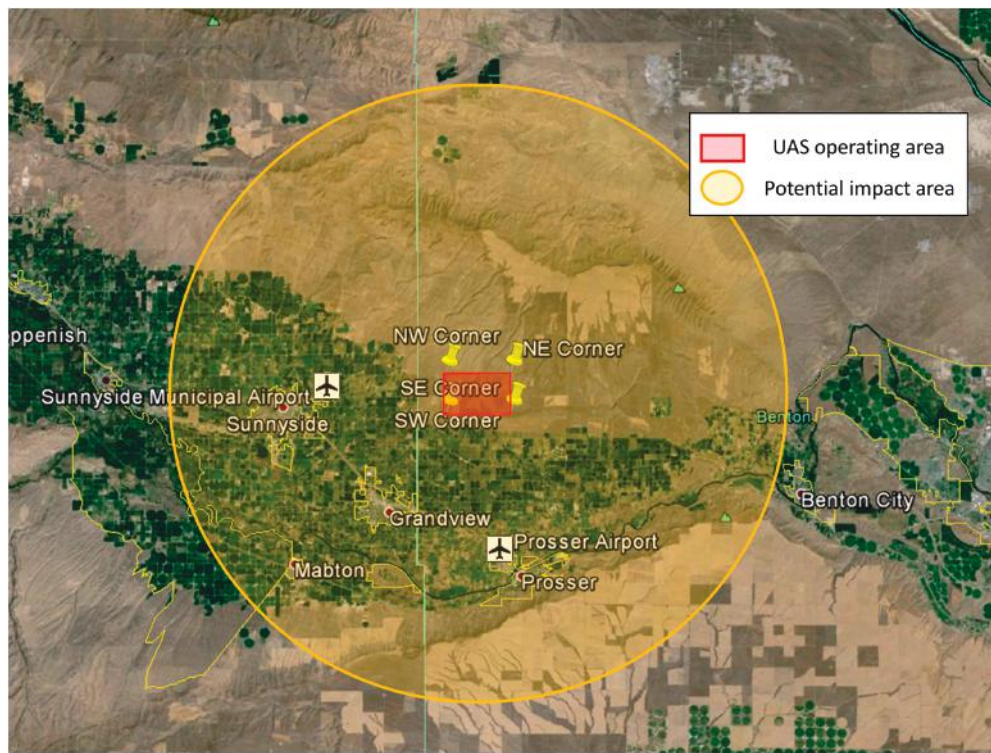


Figure 6. UAS operating area and potential impact area with respect to nearest airports (Sunnyside Municipal Airport and Prosser Airport).

not equipped with any type of transponder and is generally difficult to see.

The example operating area for this mission is near the city of Sunnyside, Washington in the United States. Figure 6 illustrates the operating area as well as potential impact area calculated for the worst-case scenario due to the general system failure.

To determine the population density near the UAS operating area, we will use the data available from the US Census Bureau. The potential impact area has 1749.7 km<sup>2</sup>. Population and housing unit density calculated in the area is therefore 19.89 people km<sup>-2</sup> and 5.93 housing-units km<sup>-2</sup>, respectively. Estimating that the average person spends not more than 10% of their time outdoors, 10% of the population will be considered pedestrians, and the remaining 90% will be divided among the housing units. This estimation gives a pedestrian density of 1.99 people km<sup>-2</sup>, and the average housing unit has 3.02 people in every building. The forward-facing areas of the UA (area likely to impact an obstacle) are mostly foam with no sharp surfaces, therefore we assume fatality when UA collides with a pedestrian and building to be  $5 \times 10^{-2}$  and  $1 \times 10^{-3}$  (aircraft penetrates 10% of the time and in those cases fatality is of people inside is  $1 \times 10^{-2}$ ), respectively.

The operating area is within the proximity of both Sunnyside Municipal Airport (K1S5) and Prosser Airport (KS40), so there are potential interactions between the UAS and the transient aircraft near the airport. From the airport database, the transient aircraft category was assumed to be general aviation only. Although the operating altitude of the Skywalker 1900 is relatively low compared to the typical airport-approach altitude profile, we still consider a portion (50%) of air traffic to be within the operation altitude of Skywalker 1900. This is further justified by the fact that some of the aircraft in this area are used for agricultural use such as crop dusting and therefore operate at low altitudes. Based on the air traffic information from two airports, air traffic density is estimated to be  $3.54 \times 10^{-4}$  aircraft km<sup>-3</sup>.

The input parameters necessary for this risk assessment are summarized in Table 1.

### 5.1.2 Risk assessment results

Using these parameters, the model predicts values shown in Table 2. The first two columns are the values as described in the risk model section. Recall that these are defined as a per hour rate of occurrence. Because the mission persists for  $M_L$  hours, the number of occurrences during the mission can be obtained by multiplying by  $M_L$ . The resulting per mission rate can then be inverted to obtain the number of

**Table 1.** Risk assessment inputs for the environmental monitoring scenario

Parameter	Value
UAS	
$V_{ua}$	20.6 m s <sup>-1</sup>
$\phi_{ua}$	0.44 m <sup>2</sup>
$w_{ua}$	1.9 m
$L_{ua}$	1.2 m
$\gamma$	5°
$\lambda$	0.1
$\epsilon_{ua/o}$	0
$\epsilon_{ua/ua}$	0
$z_{max, fleet}$	122 m
$z_{min, fleet}$	0 m
$M_L$	0.3 h
Operating area	
$N_{ua}$	2
$A_{ops}$	1749.7 km <sup>2</sup>
$\sigma_b$	5.93 housing-units km <sup>-2</sup>
$A_b$	200 m <sup>2</sup>
$H_b$	5 m
$D_{bldg}$	$1 \times 10^{-3}$ fatalities strike <sup>-1</sup>
$\sigma_p$	1.99 people km <sup>-2</sup>
$H_p$	1.75 m
$R_p$	0.25 m
$D_{ped}$	$5 \times 10^{-2}$ fatalities strike <sup>-1</sup>
Transient aircraft	
$\rho_o$	$3.54 \times 10^{-4}$ aircraft km <sup>-3</sup>
$V_o$	222 m s <sup>-1</sup>
$\phi_o$	80 m <sup>2</sup>
$P_o$	45 people aircraft <sup>-1</sup>
$\epsilon_o$	0.05

missions between occurrences. This value is shown in the third column.

The interesting result is the order of magnitude difference in fatalities due to midair collisions (1 every 65 641 years) and general system failures (1 every  $1.28 \times 10^6$  years). Although the operation expects 1 fatality every 62,433 years, the cause of this is most likely due to a midair (either transient or in-fleet) collision rather than a general system failure. Tracing the cause further back, in the already unlikely situation of a midair collision causing a fatality, this midair collision is mostly a transient aircraft collision instead of an in-fleet collision ( $F_{transient}$  is more than three times higher than  $F_{fleet}$ ). This stems from the fact that operating area is near airports and potential interaction between transient aircraft and UA is more likely to happen.

These results suggest that more lives can be saved by spending more time and effort into collision avoidance technologies than making UAS more robust and less susceptible to general system failures. Installing a transponder would be an effective solution to mitigate relatively high

**Table 2.** Risk assessment outputs for the environmental monitoring scenario

Parameter	Value	Equivalent representation
$F_{transient}$	$7.62 \times 10^{-6}$ collisions $h^{-1}$	1 transient collision every $1.97 \times 10^5$ missions
$F_{fleet}$	$2.45 \times 10^{-6}$ collisions $h^{-1}$	1 in-fleet collision every $6.13 \times 10^5$ missions
$F_{ped,p}$	$2.07 \times 10^{-5}$ strikes $h^{-1}$	1 pedestrian strike due to general failure every 72 358 missions
$F_{ped,midair}$	$1.81 \times 10^{-10}$ strikes $h^{-1}$	1 pedestrian strike due to midair collision every $8.28 \times 10^9$ missions
$F_{bldg,p}$	0.0014 strikes $h^{-1}$	1 building strike due to general failure every 1088 missions
$F_{bldg,midair}$	$2.41 \times 10^{-8}$ strikes $h^{-1}$	1 building strike due to midair collision every $6.22 \times 10^7$ missions
$F_{ped}$	$2.07 \times 10^{-5}$ strikes $h^{-1}$	1 pedestrian strike every 72 357 missions
$F_{bldg}$	0.0014 strikes $h^{-1}$	1 building strike every 1088 missions
$F_{fat,p}$	$1.17 \times 10^{-6}$ fatalities $h^{-1}$	1 fatality due to general failure every $1.28 \times 10^6$ missions
$F_{fat,midair}$	$2.29 \times 10^{-5}$ fatalities $h^{-1}$	1 fatality due to midair collisions every 65 641 missions
$F_{fat}$	$2.40 \times 10^{-5}$ fatalities $h^{-1}$	1 fatality every 62 433 missions

transient aircraft collision rate as it aids other aircraft in sensing the UA and avoiding collisions.

### 5.2 Scenario 2: urban patrol

The previous example represented the type of operation for which UAS is a reasonably safe solution. The following example will demonstrate why many other suggested uses for UAS are expected to be less viable in near term from the safety perspective. While they may have technical merit and

excellent potential benefits, risk analysis reveals significant safety issues that will prevent regulatory approval and public acceptance. One such application is the use of UAS to patrol urban environments to provide traffic monitoring, law enforcement surveillance, antiterrorist intelligence, and other services. The idea is that UAS can be used to provide persistent surveillance or monitor over areas of interest such as harbors, airports, and highways. This application has been proposed and explored by some governmental agencies (McCormack, 2008).

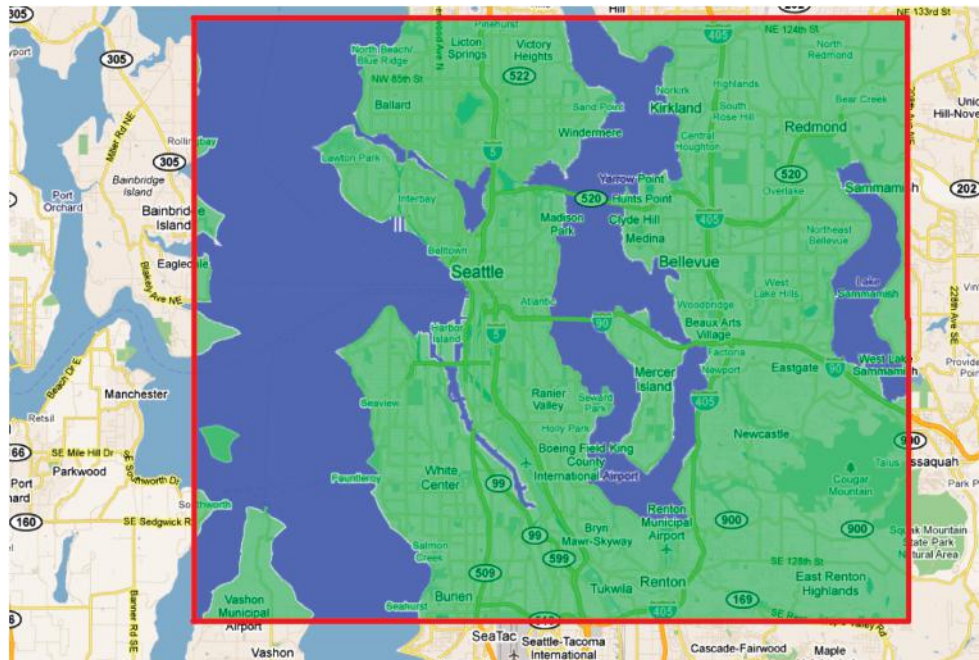


**Figure 7.** Total operating area for urban patrol UAS team. Risks are separately computed on land-based environments and marine environments.



5.2.1 UAS properties, operating area, and transient aircraft

Several case studies and trials have selected MLB Company’s BAT 3 UAV for traffic monitoring projects, so its specifications will be used here in this scenario. For the operating area, the city of Seattle, Washington in the United States will be used as an example city. The total operating area will be broken in two areas: land based environments and marine environments. These areas are shown in Figure 7. To cover this area, it is assumed that four UAS are dedicated to patrolling the total area 24 h a day, 7 days a week, for 1 year. Therefore, the definition of a single mission for this scenario is four vehicles operating continuously for 1 year. The team will be operated in an altitude range of 152 m (500 ft) to 914 m (3000 ft). The population information of the operating area will be based on data available from US Census Bureau. Finally, the air traffic densities are found from Flight Explorer Personal Edition (Real-time air traffic tracking database).

The specifications as well other relevant input parameters necessary for this risk assessment are tabulated in Table 3.

5.2.2 Risk assessment results

The results of this risk assessment are summarized in Table 4.

The most striking result of this analysis is the high level of risk this operation incurs. Due to the high density of people and buildings, both pedestrians and building strikes are virtually guaranteed over the course of 1-year mission duration. In total, there are over two fatalities expected each mission. From the analysis, it was revealed that the causes of these fatalities are mostly due to the unreliability of the UAS rather than midair collisions ( $F_{fat,p} \approx 9F_{fat,midair}$ ).

It should be noted that the above scenario assumed a set of nonredundant vehicles that are operated over sensitive areas with no planned emergency procedures. Perhaps

Table 3. UAS specification for urban patrol risk assessment

Parameter	Value
$V_{ua}$	26 m s <sup>-1</sup>
$\phi_{ua}$	0.11 m <sup>2</sup>
$w_{ua}$	1.83 m
$L_{ua}$	1.43 m
$\gamma$	3.18°
$\lambda$	0.001
$\epsilon_{ua/o}$	0
$\epsilon_{ua/ua}$	0.9
$z_{max, fleet}$	914 m (3000 ft)
$z_{min, fleet}$	152 m (500 ft)
$A_{ops, fleet}$	970.9 km <sup>2</sup>

unsurprisingly, this results in a predicted high level of fatalities. The results of this analysis perhaps motivate a more structured and planned approach to integration of UAS into operations over populated areas such as this. Carefully selecting flight paths and operating areas along with additional safety checks to increase UAS reliability could mitigate these risks significantly. The conclusion to draw from this analysis is not that unmanned systems are infeasible for this type of mission but rather that UAS with higher reliability and more carefully planned operating procedures should be utilized to bring risk levels down to acceptable levels. This illustrates how this risk assessment tool and framework can be used to identify ways to increase safety for a given UAS mission.

6 CONCLUSION

In this chapter, motivations for risk analysis, risk factors associated with its operation, and finally methodologies to

Table 4. Risk assessment outputs for the urban patrol scenario

Parameter	Value	Equivalent representation
$F_{transient}$	$2.54 \times 10^{-7}$ collisions h <sup>-1</sup>	1 transient collision every 448 missions
$F_{fleet}$	$4.01 \times 10^{-7}$ collisions h <sup>-1</sup>	1 in-fleet collision every 284 missions
$F_{ped,p}$	$8.28 \times 10^{-5}$ strikes h <sup>-1</sup>	1 pedestrian strike due to general failure every 1.3 missions
$F_{ped,midair}$	$5.88 \times 10^{-10}$ strikes h <sup>-1</sup>	1 pedestrian strike due to midair collision every 193 926 missions
$F_{bldg,p}$	0.01 strikes h <sup>-1</sup>	1 building strike due to general failure every 0.01 missions
$F_{bldg,midair}$	$9.62 \times 10^{-8}$ strikes h <sup>-1</sup>	1 building strike due to midair collision every 1185 missions
$F_{ped}$	$8.28 \times 10^{-5}$ strikes h <sup>-1</sup>	1 pedestrian strike every 1.4 missions
$F_{bldg}$	0.01 strikes h <sup>-1</sup>	1 building strike every 0.01 missions
$F_{fat,p}$	0.0002 fatalities h <sup>-1</sup>	1 fatality due to general failure every 0.43 missions
$F_{fat,midair}$	$2.97 \times 10^{-5}$ fatalities h <sup>-1</sup>	1 fatality due to midair collisions every 3.8 missions
$F_{fat}$	0.0003 fatalities h <sup>-1</sup>	1 fatality every 0.4 missions

quantitatively assess the potential risk to the public were presented. Although it is difficult to predict the exact form of regulations in the future, it is safe to say that the primary goal of those regulations will always be to ensure the safety of the public.

Development of effective SAA and C2 technologies are critical to ensure the safe interaction between manned aviation and UAS. Collision avoidance or separation systems such as TCAS and ADS-B may also be required for certain types of UAS operation. As seen in example scenarios, incorporating these elements could serve to ameliorate concerns about manned and unmanned aircraft coexisting in shared airspace as they can lower the risks for potential midair collisions and subsequent fallout during the operation.

Finally, from a certification and engineering standpoint, to ensure safe integration of UAS in the NAS, a risk analysis of the critical hazards such as midair collisions and ground impacts must be considered. The risk assessment framework presented in this chapter is designed to be a conservative and easily accessible method to estimate the risk to human life incurred from a given UAS operation. Although, the model presented here has several limitations (such as assuming the use of single type of UAS for the entire operation) the model can be given even greater flexibility by adding functionalities to accommodate missions that are more complex. A higher fidelity risk analysis should include the fact that aircraft are typically following predefined and carefully selected flight paths to mitigate some of the risk. In addition, for flights beyond 5 nmi from an airport, it is unlikely that midair collisions will be a factor due to low traffic density. The current risk model conservatively assumes a uniform density distribution and spatial flight spacing. In any situation, it is important for an operator or regulator to develop and use an appropriate model depending on the objectives and requirements for the risk analysis.

## NOTATION AND NOMENCLATURE

$A_b$	average building area
ADS-B	Automatic Dependent Surveillance – Broadcast
$A_{L_{Hb}}, A_{L_{Hp}}$	collision area for buildings and pedestrians in a horizontal crash (due to system failure)
$A_{L_{Vb}}, A_{L_{Vp}}$	collision area for buildings and pedestrians in a vertical crash (due to midair collision)
$A_{ops}$	operating area
$C_{midair}$	rate of aircraft crashes due to midair (transient and in-fleet) collisions
C2	command and control
$D_{bldg}$	expected number of fatalities when a UA collides with a building
$D_{ped}$	expected number of fatalities when a UA collides with a pedestrian

FAA	Federal Aviation Administration
$F_{fat}$	fatalities per flight hour
$F_{fat,p}$	fatalities due to system failures
$F_{fat,midair}$	fatalities due to midair collisions
$F_{ped}$	collision rate of UA fleet with pedestrian per hour
$F_{bldg,midair}$	collision rate with buildings due to midair collision
$F_{bldg,p}$	collision rate with buildings due to system failure
$F_{ped,midair}$	collision rate with pedestrians due to midair collision
$F_{ped,p}$	collision rate with pedestrians due to system failure
$F_{bldg}$	collision rate of UA fleet with buildings per hour
$F_{fleet}$	collision rate of UA fleet of other UA within fleet per flight hour
$\tilde{F}_{transient}$	collision rate of a single UA w/o avoidance & stationary transient aircraft
$\tilde{F}_{transient}$	collision rate of UA w/o avoidance & moving transient aircraft
$F_{transient}$	collision rate of UA with transient aircraft per hour
$H_b$	average building height
$H_p$	average pedestrian height
$L_{ua}$	length of UA
$M_L$	mission length
NAS	National Airspace System
$N_{ua}$	number of UA in fleet
$P_O$	average number of passengers on a transient aircraft
$R_p$	radius of a pedestrian
SAA	sense and avoid
TCAS	Traffic Alert and Collision Avoidance System
UAS	unmanned aircraft system
$w_b$	average width of buildings
$w_{ua}$	wingspan of UA
$z_{max}, z_{min}$	maximum and minimum altitude of operating area
$\alpha$	number of midair collisions predicted by the risk model
$\gamma$	glide angle of UA
$\rho_O, \rho_{ua}$	density of transient aircraft and UA, respectively
$\phi_{col}$	Instantaneous collision area
$\phi_O, \phi_{ua}$	frontal area of a transient aircraft and UA
$\epsilon_O$	ability of transient aircraft to avoid collisions with UA
$\epsilon_{ua/O}$	ability of UA to avoid collisions with transient aircraft
$\epsilon_{ua/ua}$	ability of UA to avoid collisions with other UA in fleet
$\eta_{ops}$	volume of entire operating space of mission
$\eta_{fleet}$	volume of only operating space where UA fleet exists
$\lambda$	UAS midair system failure rate
$\sigma_b, \sigma_p$	buildings and pedestrian densities

## REFERENCES

- Accident Investigation Board (n.d.) *United States Air Force Class A Aerospace Mishaps*, SL-1 Accident Investigation Board.
- Anno, J. (1982) Estimate of human control over mid-air collisions. *J. Aircr.*, 86–88.

- Anon. (2011) *Code of Federal Regulations, Title 14 Aeronautics and Space, Part 91 General Operating and Flight Rules*, United States Government, Washington DC.
- Burke, D. (2010) *System Level Airworthiness Tool: A Comprehensive Approach to Small Unmanned Aircraft System Airworthiness*, North Carolina State University.
- Clothier, R.A., Williams, B.P., Coyne, J., Wade, M., and Washington, A. (2015) *Challenges to the Development of an Airworthiness Regulatory Framework for Unmanned Aircraft Systems*, Australian Aerospace Congress, Melbourne.
- Clothier, R.A., Williams, B.P., and Fulton, N. L. (2015) Structuring the safety case for unmanned aircraft system operations in non-segregated airspace. *Saf. Sci.*, **79**, 213–228.
- Clothier, R., Williams, B., and Washington, A. (2015) *Development of a Template Safety Case for Unmanned Aircraft Operations Over Populous Areas*, SAE International.
- Dolbeer, R., Wright, S., Weller, J., and Begier, M. (2009) *Wildlife Strikes to Civil Aircraft in the United States 1990–2008*, Animal and Plant Health Inspection Service and Federal Aviation Administration.
- Federal Aviation Administration (2013) *FAA's Roadmap for Integration of Civil Unmanned Aircraft Systems (UAS) in the National Airspace System (NAS)*, Federal Aviation Administration, Washington, DC.
- Herz, R. (2008) *Assessing the Influence of Human Factors and Experience on Predator Mishaps*, Northcentral University.
- Lum, C.W., Carpenter, B., Rodriguez, A., and Dunbabin, M. (2015) Automatic wildfire detection and simulation using optical information from unmanned aerial systems, *Proceedings of the 2015 SAE Aerotec Conference*. Seattle.
- Lum, C.W., Gauksheim, K.R., Vagners, J., and McGeer, T. (2011) Assessing and estimating risk of operating unmanned aerial systems in populated areas, *Proceedings of the AIAA Aviation Technology, Integration, and Operations Conference*.
- Lum, C.W., Rysdyk, R.T., and Pongpunwattana, A. (2005) Autonomous airborne geomagnetic surveying and target identification, *Proceedings of the AIAA Infotech@Aerospace Conference*, Arlington.
- Lum, C.W. and Vagners, J. (2009) A modular algorithm for exhaustive map searching using occupancy based maps, *Seattle, Proceedings of the AIAA Infotech@Aerospace Conference*, Seattle.
- Lum, C.W. and Waggoner, B. (2011) A risk based paradigm and model for unmanned aerial systems in the national airspace, *Proceedings of the AIAA Infotech@Aerospace Conference*, St. Louis.
- McCormack, E.D. (2008) *The Use of Small Unmanned Aircraft by the Washington State Department of Transportation*, Washington State Transportation Center (TRAC), Seattle.
- McGeer, T. (1994) *Aerosonde Hazard Estimation*, Aerovel Corporation.
- McQuarrie, J. and Simon, D. (1997) *Physical Chemistry: A Molecular Approach*, University Science Books.
- U.S. Department of Defense, (1980) *MIL-STD-1629A – Procedures For Performing A Failure Mode, Effects And Criticality Analysis*, U.S. Department of Defense, Washington, DC.
- U.S. Department of Transportation (2013) *Unmanned Aircraft System (UAS) Service Demand 2015–2035: Literature Review & Projections of Future Usage*, U.S. Department of Transportation.
- Vagners, J., McGeer, T., and Newcome, L. (1999) *Quantitative Risk Management as a Regulatory Approach to Civil UAVs*, International Workshop on UAV Certification, Paris.
- Weibel, R. E. and Hansman, R. J. (2005) *Safety Consideration for Operation of Unmanned Aerial Vehicles in the National Airspace System*, MIT International Center for Air Transportation, Cambridge.
- Williams, B.P., Clothier, R.A., Fulton, N., Lin, X., Johnson, S. and Cox, K. (2014) *Building the Safety Case for UAS Operations in Support of Natural Disaster Response*, Atlanta, Proceedings of the AIAA Aviation Technology, Integration, and Operations Conference.